# Photochemical Etching of Carbonyl Groups from a Carbon Matrix: The (001) Diamond Surface

L. Weston, J. E. Downes, C. G. Baldwin, E. Granados, Sherif Abdulkader Tawfik, X. Y. Cui, C. Stampfl, and R. P. Mildren

Phys. Rev. Lett. **122**, 016802 — Published 8 January 2019

DOI: 10.1103/PhysRevLett.122.016802

# Photochemical etching of carbonyl groups from a carbon matrix: the (001) diamond surface

L. Weston,[1,2] J. E. Downes,[1] C. G. Baldwin,[1] E. Granados,[1] Sherif Abdulkader Tawfik,[3] X. Y. Cui,[4] C. Stampfl,[2] and R. P. Mildren[1]
[1]*MQ Photonics Research Centre, Department of Physics and Astronomy, Macquarie University, New South Wales 2109, Australia*
[2]*School of Physics, The University of Sydney, Sydney, New South Wales 2006, Australia*
[3]*School of Science, RMIT University, Melbourne, 3001, Australia and*
[4]*Australian Centre for Microscopy and Microanalysis, School of Aerospace, Mechanical and Mechatronic Engineering, The University of Sydney, New South Wales, 2006, Australia*
(Dated: December 10, 2018)

The surface of diamond is reported to undergo non-ablative photochemical etching when exposed to ultraviolet (UV) radiation which allows controlled single and partial layer removal of lattice layers. Oxygen termination of surface dangling bonds is known to be crucial for the etching process, however the exact mechanism of carbon ejection remains unclear. We investigate the interaction of UV laser pulses with oxygen-terminated diamond surfaces using atomic-scale surface characterization combined with first-principles time-dependent density functional theory calculations. We present evidence for laser-induced desorption (LID) from carbonyl functional groups at the diamond {001} surface. The doubly-bonded carbonyl group is photoexcited into a triply-bonded CO-like state, including scission of the underlying C – C bonds. The carbon removal process in LID is atom-by-atom; therefore, this mechanism provides a novel "top-down" approach for creating nanostructures on the surface of diamond and other carbon-containing semiconductors.

PACS numbers:

Recently, a novel 2-photon laser induced desorption (LID) phenomenon has been reported for diamond surfaces exposed to nanosecond ultraviolet (UV) pulses with incident fluence well below the threshold for laser ablation [1–5]. This "cool-etching" phenomenon appears to have a number of advantages over traditional ablative laser-machining (for which the minimum etch rates are around 10 nm/pulse); most notably, the LID process has no intensity threshold [3] and allows for carbon removal rates as low as $3\times10^{-9}$ nm/pulse for low incident fluence [6].

To date, a number of key features of LID have been characterized; in particular, the nonlinear nature of the underlying electronic excitation is evidenced by the dependence of the desorption rate on the intensity of the incident pulse [3, 7]. The surface two-photon absorption cross-section – evaluated based on the LID etch rates – is close to 25-times higher than that of bulk diamond [4, 8]; moreover, the threshold-free nature and observed dependence on the polarization of incident photons [4, 5] points to a surface-specific multi-photon-excited desorption mechanism. Given that etching of the O-terminated diamond surface is quenched in vacuum [2], it seems likely that carbon removal involves laser induced carbon monoxide (CO) desorption. However, despite extensive characterization of the LID process and a number of proposed models for the mechanism [1–5], the process is poorly understood. Determination of the mechanism is made difficult, in contrast to ablation, by the short time and length scales upon which desorption occurs and which are especially challenging to access experimentally. The current lack of understanding suggests that a microscopic and quantum mechanical approach is needed to fully understand the underlying photochemical reaction.

In this Letter, we report evidence for the atomic nature of the ejection process and theoretical study of the LID mechanism. Atomic-force microscopy (AFM) measurements are used to show the removal of a single atomic layer after laser exposure, confirming the localized nature of the optical ejection process. Using time dependent density functional theory (TDDFT) calculations to explicitly model the laser – surface interaction, we investigate the fundamental mechanism of LID at the diamond surface. It is found that UV irradiation leads to an electronic excitation of surface carbonyl groups into a CO-like state, facilitating the subsequent desorption of gas-phase CO species. This photochemical mechanism for LID foreshadows a highly promising optical method for atom-scale surface manipulation of diamond.

The experiments investigated fluence doses for etching depths corresponding to removal of several nanometers to a single and partial layer. As shown in Fig. 1(a), trenches of width 3.2 $\mu m$ (full-width half maximum) were etched into the face of an O-terminated (100) surface of single crystal diamond using a repetitively pulsed from a nanosecond deep-UV (4.5 eV) laser focused onto the sample by a cylindrical lens. By exposing the surface to a selected number of sub-ablation-threshold pulses and selecting a zone away from the beam axis, it was possible to obtain select regions that correspond to a re-

moval of single monolayers. Depth profiles were measured using an atomic force microscope in contact-mode. Our theoretical calculations are based on density functional theory (DFT). To study the ground state properties of diamond surface layers we use DFT within the generalized Kohn-Sham scheme [9], as implemented in the VASP package [10]. The effects of exchange and correlation are calculated using the generalized gradient approximation (GGA) of Perdew, Burke and Ernzerhof (PBE) [11]. The valence electrons are separated from the core by use of projector-augmented wave pseudopotentials (PAW) [12]. For the present calculations, the C $2s^2 2p^2$, O $2s^2 2p^4$, and H $1s^1$ electrons are treated explicitly. The energy cutoff for the plane wave basis set is 500 eV. Our optimized GGA lattice constant for bulk diamond is 3.83 Å; this relaxed structure is used to generate the subsequent supercell geometries. For the 8-atom primitive cell a 6×6×6 **k**-point grid was used for integrations over the Brillouin zone (BZ); for larger supercells an equivalent sampling of the BZ was used. To study the interaction of the laser pulses with the O-terminated diamond surface, we perform dynamical simulations within TDDFT using the octopus code [13]. For the TDDFT simulations, geometries are taken from relaxations performed in VASP. The laser-surface interaction is modelled explicitly using simulated laser pulses with different photon energy, intensity and pulse duration. The time propagator was approximated using the exponential midpoint rule. The time step for the propagations was 0.00057 fs. We use a real space grid with spacing 0.23 Å, and a 30 Å×30 Å×30 Å simulation box with absorbing boundaries. Spin polarization was taken into account.

*Experimental results.* Six trenches were LID-etched for exposures comprising of between $10^5$ to $10^8$ pulses. These were first profiled using laser interferometry (Fig. 1(b)) to calibrate the system etch rate which was determined to be $1.3 \times 10^-6$ nm per pulse at the deepest point in the trench (ie., on the beam axis) for a fluence of 0.02 J/cm$^2$ incident on the focusing lens. Fig. 1(c) shows a high-resolution AFM profile for an exposure of $2.5 \times 10^6$ pulses at a point $1 - 2$ mm from the beam axis. The AFM image and corresponding cross-section indicates an etch depth corresponding to 360 pm of the same order as the diamond lattice constant. This result is shows unequivocally that the etching process occurs atom-by-atom (as opposed to laser ablation which is a collective process), and suggests an atomic-scale laser-surface interaction.

*Theoretical results.* Diamond crystallizes in a face centred cubic structure, in which each C atom is tetrahedrally coordinates to four neighbouring C atoms. This geometry arises from the hybridization of C $2s$ and C $2p$ atomic functions; the four $sp^3$ hybrids form $\sigma$-bonded molecular orbitals which comprise the valence band of bulk diamond, and the corresponding antibonding states comprise the bulk conduction band. As a result of the strong covalent interaction, the $sp^3$ $\sigma - \sigma^*$ splitting is

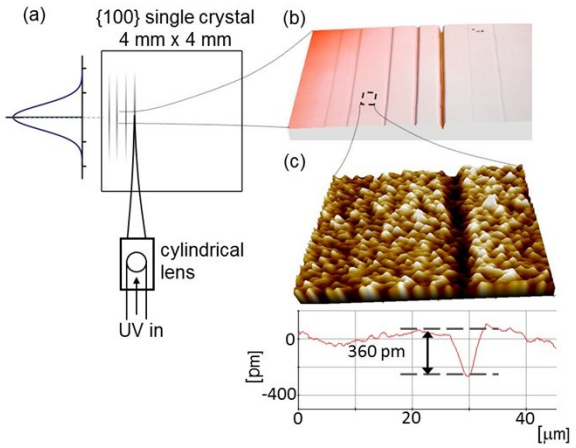


FIG. 1: UV-induced LID of a (100) single crystal diamond. (a) 266 nm laser pulses of 5 ns duration are focused using a cylindrical lens ($f$ = 25 mm) to etch trenches of full-width half-maximum 3.2 × 3000 $\mu$m. (b) Repetitive pulse exposures at 125 kHz and of on-axis fluence 0.02 J/cm$^2$ provided controlled etch depths from partial layer removal to hundreds of layers using durations up to 80 minutes. (c) Atomic force microscopy image (45 × 45$\mu$m) of the surface for a 4 minute exposure at 0.01 J/cm$^2$ yielded an average etch depth approximately equal to the diamond lattice constant ($a$ = 0.357nm).

about 5.5 eV making diamond a wide band gap insulator. For the cubic {001} face, the surface carbon species are 2-fold coordinated to the layer below, and can therefore be thought of as having two $sp^3$ dangling bonds per surface carbon; however, local $sp^2$ re-hybridization at the terminating carbon site facilitates the adsorption of doubly bonded carbonyl species at the surface [14]. A carbonyl terminating species on a (001)-surface is shown in Fig. 2(a), where the C – O double bond is directed along the [001] direction. The {001} surface also supports a bridging (ether) termination; however, X-ray experiments have indicated a reduced number of carbonyl sites compared to bridging sites post etching, suggesting a preferential (or even exclusive) CO removal from carbonyl sites [5]. Moreover, post-etch diamond surfaces exhibit strong {111}-like faceting [5], indicating this surface is resistant to etching ; importantly, the {111} surface cannot support carbonyl groups, explaining the etch resistance of this surface. For these reasons, we focus on the carbonyl surface species for the present study.

As a first step to understanding the laser-induced desorption of CO from a diamond (001) surface, we compare the electronic structure of an extended carbonyl-terminated (001) slab with that of an isolated CO molecule. The geometry of the slab is presented in Fig. 2(b) (top view) and Fig. 2(c) (side view); we closely follow the model used in Ref. [15], with a slab having a single carbonyl-terminated (001) face (25% coverage), and with the back surface being terminated with hydrogen in order to passivate dangling bonds. Repeating lay-

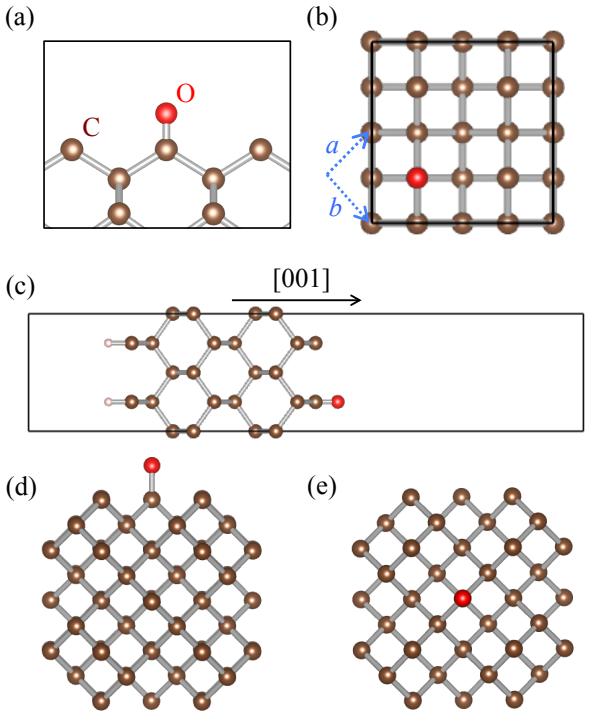


FIG. 2: (a) A diamond (001) surface with an adsorbed O-atom at the carbonyl site. (b) The supercell used in the electronic structure calculations viewed along the [00$\bar{1}$] direction. The (001) surface has a single adsorbed atom at the carbonyl site, representing 25% surface coverage. The in-plane dimensions of the supercell are $2\sqrt{a} \times 2\sqrt{b}$, the lattice vectors of the primitive cell are indicated. (c) Side view of the supercell used in the electronic structure calculations. Carbon atoms are represented by brown spheres, O are red, H are white.

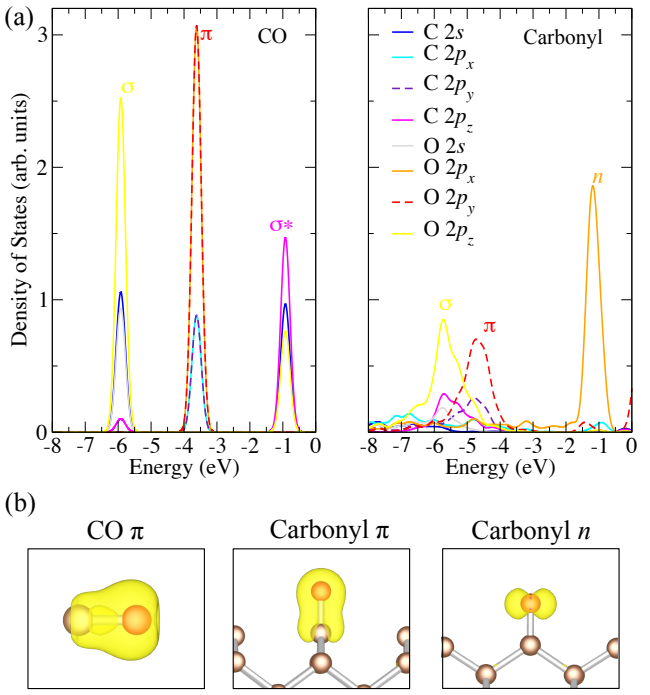


FIG. 3: (a) The site-projected partial density of states for an isolated CO molecule (left) and CO chemisorbed at the carbonyl site of a diamond (001) surface (right). (b) Charge density isosurface for the doubly degenerate $\pi$-bonding state of the CO molecule (left), and the singly degenerate $\pi$-bonding and lone pair ($n$) states of the chemisorbed carbonyl. Carbon atoms are represented by brown spheres, O are red, and the isosurface is yellow. The value of the isosurface is set to 10% of the maximum value.

ers are separated by a vacuum region of approximately 13 Å. The electronic structure is investigated in Fig. 3, where the partial and site-projected partial density of states (pdos) is plotted for a CO molecule and a (001) carbonyl terminating CO-species. We consider, for the sake of our arguments, that the carbonyl species represents a strongly chemisorbed CO molecule, and therefore we plot the pdos projected onto the O atom and the C atom directly (doubly) bonded to O; we focus on the frontier orbitals around the highest occupied molecular orbital (HOMO). The pdos in this region for the isolated CO molecule is characterized by three characteristic features: the deepest peak shown (6 eV below the HOMO) is the C – O $\sigma$-bonding peak, having $2s$ and $2p_z$ character (for a C – O bonding axis along $z$); the large peak centred almost 4 eV below the HOMO corresponds to the doubly degenerate $\pi$-bonding manifold, originating from the overlap of the $2p_x$ and $2p_y$ atomic functions of the C and O atoms; the HOMO itself corresponds to the antibonding $\sigma^*$ state, which is occupied as CO does not satisfy the octect rule. The pdos of the carbonyl exhibits several distinct features when compared to that of the CO molecule. Unlike the $sp$ system exhibited by C in the CO molecule, the chemisorbed C atom is $sp^2$ hybridized; two of the $sp^2$ hybrids exhibit a $\sigma$-bonding interaction with the substrate, and the third $sp^2$ hybrid forms a $\sigma$ bond with the above O $2p_z$ atomic orbital, which is present in the pdos as the peak nearly 6 eV below the HOMO. For the carbonyl group, the doubly degenerate $\pi$-bonding manifold of the CO molecule is split into a singly degenerate $\pi$-bonding state around 5 eV below the HOMO (labelled $\pi$), and a non-bonding lone pair state ($n$), which is the HOMO of the system. Importantly, as is clearly shown by the pdos, the CO molecule and carbonyl group represent triply- and doubly-bonded C – O systems, respectively.

As has now been demonstrated, a fundamental difference in the bonding environment between the CO molecule and the chemisorbed carbonyl group, is the splitting of the doubly degenerate $\pi$ manifold of the CO molecule with $sp$ hybridization, into singly degenerate $\pi$ and $n$ states ($sp^2$ hybridization); if the LID process occurs via carbonyl ejection, the laser-induced photochemical reaction must transform the carbonyl surface group into a CO-like state, i.e, a rehybridization from $sp^2$ to $sp$ bonding. To investigate the laser-induced excitation of

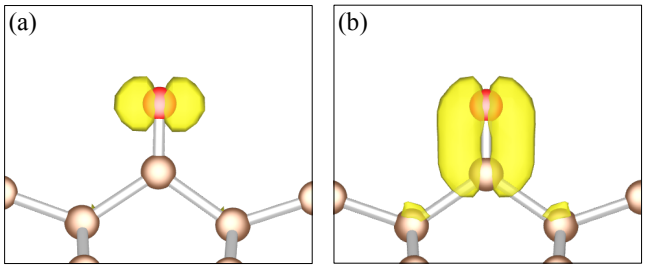


FIG. 4: (a) The O $2p$ $n$ lone pair at $t = 0$. (b) The same state is shown after applying a 4.5 eV laser pulse with intensity $3.2{\times}10^{16}$ W/cm$^2$ for 1 fs. The $n$ state transitions into a C – O $\pi$-bonding state, signalling an electronic reconstruction of the C atom from $sp^2$ to $sp$ bonding. Carbon atoms are represented by brown spheres, O are red, and the isosurface is yellow. The value of the isosurface is set to 10% of the maximum value.

the surface carbonyl group, we have performed explicit time-dependent propagation (TDDFT) of the diamond surface molecular orbitals in the presence of a strong laser field. The model system used in the TDDFT calculations is a cubic-faced diamondoid particle, as shown in Fig. 2(d) – (e). The particle has 75 C atoms and is cubic, with 6 {001} faces – to model an adsorbed carbonyl species we place a single O atom at the carbonyl site on one of the faces. We performed tests for a number of nanoparticle structures, including different O terminations and atomic relaxations, and found that our main conclusions are not sensitive to steric and other local environment effects. The use of different systems for the static and time-dependent calculations is largely a result of technical issues in using the VASP and Octopus codes; however, analysis of the pdos for these systems reveals that the local electronic structure presented in Fig. 3 for the carbonyl in the extended system is well reproduced for the diamondoid particle.

We present TDDFT results for a 4.5 eV incident pulse with a duration of 1 fs and maximum intensity of $3.2{\times}10^{16}$ W/cm$^2$. The key bonding features of the carbonyl group, namely the $\sigma$, $\pi$ and $n$ states, were monitored as the wavefunction propagated under the influence of the applied laser field. In Fig. 4(a), we plot the charge density isosurface for the $n$ state before the laser pulse. Fig. 4(b) shows the charge density isosurface of the same state after the 1 fs pulse. As can be seen, the pulse transforms the $n$ state into a C – O $\pi$-bonding molecular orbital.

Plotting the electronic states of the system reveals that the original $\sigma$ and $\pi$ states of the carbonyl group remain intact. After the pulse, the C – O system exhibits a triply bonded manifold that resembles a CO molecule-like state (Fig. 3(a)). *Importantly*, the transition from a doubly to triply bonded manifold indicates a transition from $sp^2$ to $sp$ bonding for the C atom in the carbonyl group. When the C atom of the carbonyl group is in an $sp^2$ state, there are two $sp^2$ orbitals that point directly at the $sp^3$ bonded C atoms in the layer below; these orbitals overlap to form strong $\sigma$ bonds. However, once the C atom of the carbonyl group transitions into an $sp$ state, the $sp^2$ orbitals are no longer present, and so these C – C $\sigma$ bonds cannot form. Therefore, the transition of the C – O system into an $sp$ state indicates unambigously a mechanism for scission of the underlying C – C bonds, and facilitates the desorption of a CO molecule from the surface.

This LID mechanism is reminiscent of well-known processes in organic photochemistry, whereby carbonyl containing molecules undergo various photochemical reactions under UV laser exposure [16]. Thus it represents a novel link between decades-old photochemistry and modern solid-state nanotechnology. We also note that carbonyl functional groups can, in principle, form on the surface of other carbon containing solids, for example SiC, and therefore LID could prove useful in the nanomachining of a range of hard covalent solids. Moreover, experimental and theoretical work has confirmed that carbonyl groups are stable on the zig-zag edge of graphene [17, 18]. Indeed, recent work has indicated that graphene undergoes photochemical etching in the presence of oxygen when exposed to UV radiation [19], however the mechanism for the observed etching is unclear. Given the localized and site-specific nature of the LID process, this opens up tremendous opportunities for optical manipulation of semiconductor surfaces with atomic-scale precision. With advanced atom-placement technologies based on scanning tunneling microscopy, surface adsorbates can be deposited with atomic-scale precision [20]. With the current LID mechanism, this is extended to the controlled creation of single-vacancy defects at semiconductor surfaces, which could have far-reaching applications including in quantum information science [21].

In summary, using a combination of atomic-scale surface characterization and TDDFT calculations, we have revealed the microscopic mechanism for LID at oxygen-terminated diamond (100) surfaces. The carbon ejection mechanism involves direct laser-induced excitation of surface carbonyl functional groups into a triply-bonded CO-molecule like state, including scission of the underlying C – C bonds. The site-specific nature of the carbon-removal process suggests that LID is highly promising for the "top-down", atom-scale manipulation of diamond and other carbon-containing semiconductor surfaces.

Acknowledgment - This research was sponsored by the Australian Research Council Discovery Grant (DP150102054) Scheme and the US Air Force Research Laboratory under agreement number FA2386-15-1-4075.

[1] V. V. Kononenko, M. S. Komlenok, S. M. Pimenov, and V. I. Konov, Quant. Electron. **37**, 1043 (2007).

[2] M. Komlenok, V. Kononenko, V. Ralchenko, S. Pimenov, and V. Konov, Phys. Procedia **12**, 37 (2011).

[3] R. P. Mildren, J. E. Downes, J. D. Brown, B. F. Johnston, E. Granados, D. J. Spence, A. Lehmann, L. Weston, and A. Bramble, Opt. Mater. Express **1**, 576 (2011).

[4] A. Lehmann, C. Bradac, and R. Mildren, Nat. Commun. **5** (2014).

[5] C. Baldwin, J. Downes, C. McMahon, C. Bradac, and R. Mildren, Phys. Rev. B **89**, 195422 (2014).

[6] E. Granados, D. J. Spence, and R. P. Mildren, Opt. Express **19**, 10857 (2011).

[7] V. Kononenko, V. Gololobov, M. Komlenok, and V. Konov, Laser Phys. Lett. **12**, 096101 (2015).

[8] J. Dadap, G. B. Focht, D. Reitze, and M. C. Downer, Opt. Lett. **16**, 499 (1991).

[9] W. Kohn and L. J. Sham, Phys. Rev. **140**, A1133 (1965).

[10] G. Kresse and J. Furthmüller, Phys. Rev. B **54**, 11169 (1996).

[11] J. P. Perdew, K. Burke, and M. Ernzerhof, Phys. Rev. Lett. **77**, 3865 (1996).

[12] P. E. Blöchl, Phys. Rev. B **50**, 17953 (1994).

[13] A. Castro, H. Appel, M. Oliveira, C. A. Rozzi, X. Andrade, F. Lorenzen, M. A. Marques, E. Gross, and A. Rubio, Phys. Status Solidi B **243**, 2465 (2006).

[14] P. John, N. Polwart, C. E. Troupe, and J. I. Wilson, J. Amer. Chem. Soc. **125**, 6600 (2003).

[15] T. Derry, N. Makau, and C. Stampfl, J. Phys.: Condens. Matt. **22**, 265007 (2010).

[16] T. Laue and A. Plagens, *Named organic reactions* (John Wiley & Sons, 2005).

[17] M. Ohtsuka, S. Fujii, M. Kiguchi, and T. Enoki, ACS Nano **7**, 6868 (2013).

[18] O. Hod, V. Barone, J. E. Peralta, and G. E. Scuseria, Nano Lett. **7**, 2295 (2007).

[19] N. Mitoma and R. Nouchi, Appl. Phys. Lett. **103**, 201605 (2013).

[20] P. M. Koenraad and M. E. Flatté, Nat. Mater. **10**, 91 (2011).

[21] J. Weber, W. Koehl, J. Varley, A. Janotti, B. Buckley, C. Van de Walle, and D. D. Awschalom, Proc. Natl. Acad. Sci. **107**, 8513 (2010).